

Review of low actuation voltage RF MEMS electrostatic switches based on metallic and carbon alloys

Yasser Mafinejad¹, Abbas Kouzani², Khalil Mafinezhad³

¹*School of Engineering, Deakin University, Waurn Ponds, Australia*

²*School of Engineering, Deakin University, Waurn Ponds, Australia*

³*School of Electrical Engineering, Sadjad Institute of Higher Education, Ferdowsi University, Mashad, Iran*

Abstract: Radio frequency micro electro mechanical systems (RF MEMS) have enabled a new generation of devices that bring many advantages due to their very high performances. There are many incentives for the integration of the RF MEMS switches and electronic devices on the same chip. However, the high actuation voltage of RF MEMS switches compared to electronic devices poses a major problem. By reducing the actuation voltage of the RF MEMS switch, it is possible to integrate it into current electronic devices. Lowering the actuation voltage will have an impact on RF parameters of the RF MEMS switches. This investigation focuses on recent progress in reducing the actuation voltage with an emphasis on a modular approach that gives acceptable design parameters. A number of rules that should be considered in design and fabrication of low actuation RF MEMS switches are suggested.

Keywords: RF MEMS switch, low actuation voltage, RF parameters, metallic and carbon alloys

Pregled RF MEMS elektrostatičnih stikal z nizko napetostjo vzbujanja na osnovi kovinskih in karbonskih zlitin

Izveček: Mikro elektromehanski sistemi na radijski frekvenci (RF MEMS) so omogočili razvoj novih naprav predvsem zaradi njihove visoke učinkovitosti. Obstajajo številne spodbude k uporabi RF MEMS stikal in elektronskih naprav na enem samem čipu, vendar visoka vzbujevalna napetost predstavlja problem. Z znižanjem vzbujevalne napetosti lahko RF MEMS stikala vgradimo v obstoječe naprave. Znižanje napetosti pa bo imelo velik vpliv na RF lastnosti stikal. V članku so predstavljene trenutne smernice nižanja vzbujevalne napetosti na osnovi modularnega pristopa, ki omogoča sprejemljive parametre načrtovanja. Predlagana so številna pravila, ki bi se naj upoštevala pri načrtovanju in izdelavi RF MEMS stikal.

Ključne besede: RF MEMS stikala, nizka napetost vzbujanja, RF parametri, kovinske in karbonske zlitine

* Corresponding Author's e-mail: ymafinej@deakin.edu.au

1 Introduction

Micro electro mechanical systems (MEMS) have enabled a new generation of electronic devices, particularly RF switches. MEMS switches can be employed in radio frequency (RF) circuits, and their performances could be made better than those of other standard switches such as FET, and PIN diodes [1]. This is due to their good linearity, low noise, low power consumption, high electrical isolation, and ultra wide frequency band

[2]. MEMS switches are designed to operate for DC to a few hundred GHz applications [3, 4]. For example, they can be used in cell phones, short range communication systems such as WLAN and Bluetooth [5, 6], automotive systems such as acceleration and gyro sensors [7, 8], biomedical devices such as lab-on-a-chip [9-12], and radar applications [13, 14].

RF MEMS switches can be categorized into four groups according to their types of actuation forces. The first

type is the Piezoelectric RF MEMS switches. This type of switch uses piezoelectric materials such as AlN or PZT on top of the membrane or beam. These piezoelectric materials cause an elongation and strain across the length of the piezoelectric layer and make the beam deflect by applying the voltage. The amount of force depends on the piezoelectric coefficient. Therefore, the low actuation voltage can be achieved by chosen a high piezoelectric coefficient [15-23]. The second type of MEMS switch is the electromagnetic RF MEMS switch. This type of switch uses coil on top of the membrane. The electromagnetic force is created when a DC current is applied to the coil and actuates the membrane [24-26]. The third type is the electro-thermal RF MEMS switch. The bending of the structure depends on the thermal expansion coefficient of materials. Applying a current through the resistor on top of the beam causes a thermal wave propagates and attenuates in the thickness direction and it deflects the beam. [27, 28]. The last and more applicable type is the electrostatic RF MEMS switch. This type of switch operates only based on the amount of actuation voltage and the capacitance between the transmission line and the membrane. Table 1 compares all types of the RF MEMS switch. As can be seen from the Table 1, electrostatic force performs better in all parameters except for the actuation voltage, which is very high. Although the switching time and reliability of the electrostatic MEMS switches are better than those of other types, they not compare well with other RF switches, such as semiconductor and mechanical switches [29-33].

Carbon allotropes such as graphene and carbon nano tubes have shown superior electrical and mechanical performance compared to other types of materials. Nowadays, carbon allotropes are used widely in microwaves [34, 35]. Due to the great advantage of these materials, they can be a very good candidates for development of the RF MEMS switches [36].

In the future, electronic industry will need to integrate the MEMS and electronic devices on the same substrate. Our experience with the nonlinearity and noise of amplifiers shows that applying MEMS technologies for RF components such as RF tuning filter, switches, phase shifter, and transceiver systems will provide a far better performance than the current techniques [37-42]. Moreover, this technology also provide advantages such as miniaturizing the size, enhancing signal transduction, reduced chip pin out, increasing immunity to the electromagnetic interference, reducing power loss, and offering lower cost compared with multichip implementations [43-45]. The main problem for integration of the RF MEMS electrostatic switches with the current electronic devices is their very high actuation voltage (more than 50 Volts).

Although there are some review papers and books covering RF MEMS switches, there are as yet no book or paper discussing methods developed for lowering the actuation voltage of the RF MEMS switches. The aim of this investigation is to introduce, explain and compare recent techniques and materials developed for lowering the actuation voltage of the electrostatic RF MEMS switches that can be used in IC technology (<15V).

Section 2 discusses the principles of the RF MEMS switches based on metals and carbon materials, and their main parameters. Section 3 focuses on recent methods used for lowering the actuation voltage and compares them and their effects on switch parameters.

Table 1: Comparison of different types of MEMS switch actuation

	Piezo-electric	Electro-thermal	Electro-magnetic	Electro-static
Size	Medium	Medium	Large	Small
Fabrication process	Complex	Medium	Complex	Simple
Actuation voltage	Medium	Low	Low	High
Power consumption	Medium	High	High	Low
Switching speed	Fast	Slow	Medium	Fast
Reliability	Medium	Low	Medium	High

2 Principles of MEMS switches

In order to provide a background to the RF MEMS switches, this section presents basic information on the structure, fabrication, modelling, and categorization of such switches.

2.1 MEMS switch structure

MEMS switches have different shapes. All MEMS switches have the same structure, which consists of three components [46-49], as shown in Figure 1. The first component is substrate, which is the basic element of any microelectronic device, and is used to mount a device on top of it (surface micromachining), or inside it (bulk micro machining). In order to integrate the RF MEMS switch with IC circuits, high resistivity silicon such as HR or porous silicon [50-52], is used. This is due to the high loss of normal silicon at high frequencies. The substrates that can be used in RF MEMS switches are given in Table 2. The second component is a transmission line, which is used for transferring the RF signals from the input to the output ports. The third

component is a cantilever or membrane, which are movable parts for connecting and disconnecting the signal line (dual-fixed bridge shunt switch) (Figure 1).

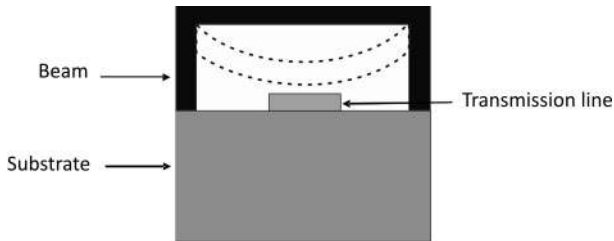


Figure 1: Structure of RF MEMS switch (dual-fixed bridge shunt switch)

Table 2: Materials used for substrate

Substrate	Quartz	Alumina (Al)	Sapphire	Silicon	Galium arsenide
Relative Permittivity	3.78	9.75	11.72	11.72	12.91

2.2 Materials of RF MEMS switches

RF MEMS electrostatic switches can be categorized, based on their materials, into two groups. The first group is the metallic MEMS switch, which uses metallic alloys such as copper, aluminium and gold. The second group is the carbon MEMS switch, based on carbon nano tube (CNT) or graphene. CNT is a type of carbon allotrope where rolled sheets of sp²-bonded graphene are shaped into a long hollow tube. CNT can be categorized into a single-wall carbon nanotube (SWCNT) and multi-wall carbon nanotube (MWCNT). Graphene is a type of carbon allotrope which can be geometrically considered as single atomic layer of carbon. The electrical and mechanical properties of these materials are superior to other materials (Table 3). Also, these materials reduce the size of switch from micro to nano meter (NEMS switches) [53-57].

Table 3: Materials for MEMS and NEMS switches

Types of switch	Material	Resistance $\mu\Omega \times \text{cm} (\rho)$	Young's modulus (GPa)
MEMS metallic switch	Copper	1.69	117
	Gold	2.2	79
	Aluminium	2.65	69
MEMS carbon switch	CNT	10	1000
	Graphene	10	1000

2.3 Fabrication of MEMS switches

MEMS switches based on metal are fabricated using two techniques. The first technique is bulk micromachining, which is based on the etching of silicon substrate and

it relies on the etch rate of the crystal direction [58]. The second technique is surface micromachining. It is based on lithography, deposition of metals and etching of sacrificial layers to release the bridge or membrane on the transmission line, and uses 5-6 masks. More information on metal-based switches fabrication is given in [59-63].

Fabrication of the RF MEMS switches based on carbon material can be achieved using three steps as described in [64, 65]. The first step is to pattern the transmission line. The second step is to grow CNT or Graphene by chemical vapour deposition [66]. The third step is to pattern metal contacts onto two edges of the beam.

2.4 MEMS model

Analysing the RF MEMS switches requires extracting the mechanical and electrical models of the switches.

Mechanical model

A comprehensive study of the dynamics and statics of MEMS switches can be found in [67-69]. Figure 2 shows the mechanical model of the RF MEMS switch. There are three types of forces involved in MEMS switches. First, the Van der Waals force, which plays an important role while the gap between the two electrodes is in the range of a few nano meters. The second force is the electrostatic force, which relies on a voltage source and a capacitor between the TL and the membrane. The third force is due to the elastic force, which is modelled as a spring and depends on the shape, material and size of the beam or the membrane.

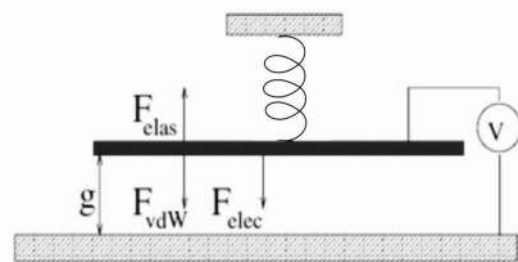


Figure 2: Mechanical model of a MEMS switch

Actuation voltage makes instability and causes the upper electrode to snap down. Another important mechanical parameter of the MEMS switch is the switching time. The switching time of MEMS switches is limited by the mechanical structure. The pull in actuation voltage ($V_{pull-in}$) and switching time (t_s) for vertical types of MEMS is as follows [70-73]:

$$V_{pull-in} = \sqrt{\frac{8kg_0^3}{27A\epsilon_0}} \tag{1}$$

$$t_s = 0.46 f^{-1} \tag{2}$$

$$f = \sqrt{\frac{k}{m}} \tag{3}$$

where k is the spring constant, g_0 is the gap between electrodes without actuation voltage, A is the overlap area between the bridge and the transmission line or the electrode, f, m is the mass of beam and f is the first resonant frequency of the beam.

Electrical model

The switch has two states: On and Off. The RF parameters of the switch, such as S_{11} and S_{21} , can be calculated by the electrical model in both states [74]. Figure 3 shows the RF MEMS shunt and series switches, which are modelled by electrical circuits. The switch is modelled by C, L, and R components. L represents the inductance of the switch, R shows the insertion loss, and C, which is the dominating parameter, represents the capacitance between the bridge and the transmission line. This capacitance has two extreme values at the up state and the down state and varies between them. The values of S_{11} and S_{21} strongly depend on the capacitance of the bridge. For example, the amount of S_{11} and S_{21} for the shunt switches are given by (4-6)

$$|s_{11}|^2 + |s_{21}|^2 = 1 \tag{4}$$

$$s_{11}(up\ state) = \frac{-j\omega C_{up} Z_0}{2 + j\omega Z_0} \tag{5}$$

$$S_{21}(down\ state) = \frac{2}{2 + j\omega C_{down} Z_0} \tag{6}$$

According to equations 1-5, table 4 summarizes the impact of physical parameters on both mechanical and electrical properties of the switch. For example, reducing the gap between the signal line and the bridge (g) reduces the actuation voltage. However, this increases the up state capacitance (C_{up}) and diminishes the isolation (S_{21}). Therefore, it reduces the bandwidth at up state (S_{21}). Moreover, although reduction of spring constant (K) reduces the actuation voltage but it reduces the resonant frequency or increasing the switching time.

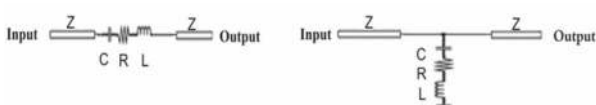


Figure 3: Series and shunt electrical model of MEMS switches

Table 4: Effects of physical parameters on the mechanical and RF properties of the switch

Physical parameters	Mechanical properties		Electrical properties	
	Vpull-in	Frequency Resonant	Up state bandwidth	Down state
Reduction of g	Reduce	Does not effect	Reduce	Does not effect
Reduction of K	Reduce	Reduce	Does not effect	Does not effect
Increase of size	Reduce	Reduce	Reduce	Increase

3 Review of low actuation voltage RF MEMS switches

As was mentioned in the previous section, MEMS switches have different parameters which should be considered in their design and fabrication. This section reviews the methods that have been used to reduce the actuation voltage while considering the requirements of other parameters of the switches as described in previous section. The methods used to reduce the actuation voltage of switches can be categorized into three groups.

3.1 Low actuation voltage based on reducing the gap

According to Table 4, reduction of the gap decreases the actuation voltage but it also deteriorates the RF parameters. The following techniques are used to reduce the actuation voltage while maintaining RF parameters at acceptable levels:

3.1.1 Matching circuit

The amount of parasitic capacitance affects negatively on the insertion loss of the MEMS switches at up state position. One effective method for compensating this capacitance is by using a matching circuit accompanied by a switch. In this way, the amount of gap can be reduced at any range. Mafinejad et al. [75-79] reported a low actuation voltage shunt capacitive contact for the frequency band of Ka to V, by using a T and π matching circuits. The T match circuit uses two short high impedance transmission lines (SHITL) before and after the switch on CPW transmission line while a π match was used only one SHITL between two switches on CPW. The SHITL can be achieved by increasing the distance between TL and the ground or narrowing the signal line of CPW (Figure 4).

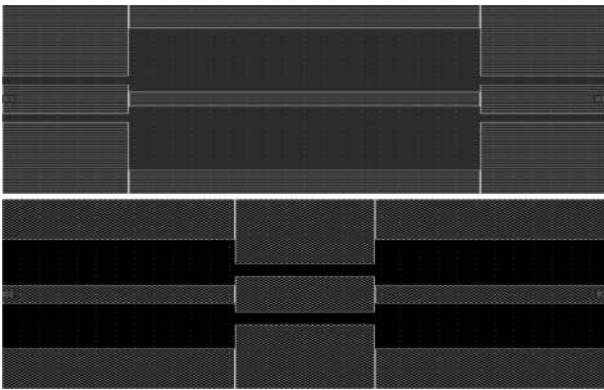


Figure 4: π and T matching circuits

3.1.2 Using pillars and an extra voltage source

The second method for reducing the actuation voltage is by using the structure which is shown in Figure 5. It consists of a beam which is anchored to a pillar at the middle whilst leaving the ends free. This method uses two separate voltage sources to provide a negative and positive voltage. This type of switch has three states: On, Off and Neutral. When voltages are applied to either of the electrodes, a large positive deflection is then noticed on one side and a smaller negative deflection of the membrane is obtained with a large contact area on the other side. This creates a large capacitance ratio for up and down state position.

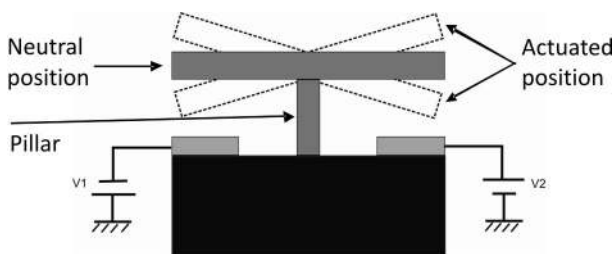


Figure 5: RF MEMS switch by using pillars and two voltage sources

Tauati et al. [80] designed a low actuation voltage (5 v) series switch that can be used for DC up to 10GHz. The switch used two pillars and four electrodes (two internal and two external). Robin et al. [81] proposed a RF MEMS SPDT switch with an actuation voltage of 20V for the frequency band of 15-30GHz. The switch consists of three pillars for the support of a gold membrane, and four electrodes (two internal and two external). Kim et al. [82] designed a Single Input Double Output (SIDO) switch from 2-10 GHz application . The actuation voltage of this switch is 15V. The switch consists of dual fixed beam and a pillar which is positioned under the beam leaving a small gap. When the SW2 changes to the ON state, SW1 is restored by the leveraging force as well as by its own stiffness. After SW2 is turned ON, the SW1 is forced to maintain higher bending stiffness

against the self-actuation power with the help of an axial force and leveraging moment.

3.1.3 Comb switches

Unlike the MEMS switches which have vertical actuation, this type of switch has a lateral actuation. The lateral switch consists of three main parts: A comb driver, which consists of stationary and movable combs to provide electrostatic force (Figure 6). The second part is a flexible structure which works as a beam or membrane of vertical switches and is connected to the driver. The third part consists of a transmission line [83-85].

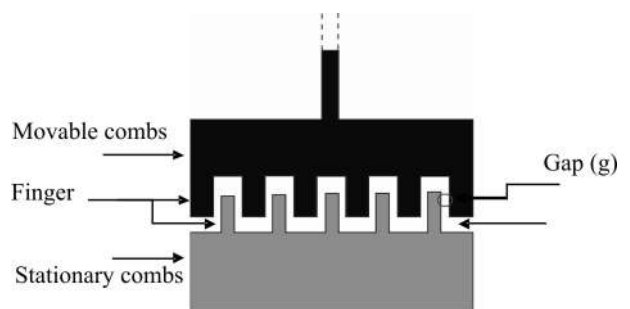


Figure 6: Comb driver

The electrostatic force (F_{es}) between two moveable and stationary combs as a result of applied voltage between them is given as:

$$F_{es} = \frac{\epsilon_0 t}{g} NV^2 + \frac{\epsilon_0 wh}{d} NV^2 \tag{7}$$

g is the gap, t is the thickness of the comb drive, d is the gap between the moveable and stationary combs, N is the number of fingers, and d is the distance between movable and stationary fingers.

Kang et al. [86] designed and fabricated Single Input 4 Output (SI4O) and SI12O RF MEMS series DC contact switches. The actuation voltage of both switches is 15V and the frequency band is DC to 10 GHz. The gap between the flexible structure and the transmission line is 2.5µm and the actuation voltage is 15V. The switching speed is 120µs and 500µs for the switch ON and OFF position. The driver uses 1200 combs and the electrostatic force is 210µN. Akira et al. [87] designed a lateral movement shunt DC switch. The total dimension of this switch is 3×1.5×0.5mm³ (the length, width and thickness respectively). The switch has a frequency band from 0 to 75 GHz and the actuation voltage is 5V. The switching time is 10.3µs. Park et al. [88] proposed a lateral movement capacitive shunt RF MEMS switch for 23.5 to 29GHz. Flexible structure is a folded beam spring. The actuation voltage of this switch is 25V and the switching time is 8ms. It used 1000 combs with a

gap of 2.1 μm. The air is used as both on and off state capacitive coupling switch instead of dielectric material.

3.2 Spring constant

According to Table 4, spring constant plays an important role on the actuation voltage of RF MEMS switches. The spring constant of MEMS switch is given by

$$K = K_{spring} + K_0 \tag{8}$$

Therefore, reduction of the spring constant can be categorized into reduction of spring constant of beam or membrane and residual stress (K_0).

3.2.1 Spring constant of beam or membrane

Beam or membrane spring constant consists of two parameters: K_{spring} which is due to material properties such as Young's modulus and shapes of the beam or membrane. A comprehensive study of low constant beams such as fixed-fixed, crab leg or folded flexures that can be used for reducing the actuation voltage is provided in [71]. Kundu et al. [89] reported a low actuation voltage RF MEMS switch with a frequency band from 5GHz to 30GHz. They introduced the concept of moving transmission line and membrane. Therefore, the equivalent spring constant of the switch follows the series spring constant rules. The actuation voltage reduced from 20V to 15V (Figure 7).

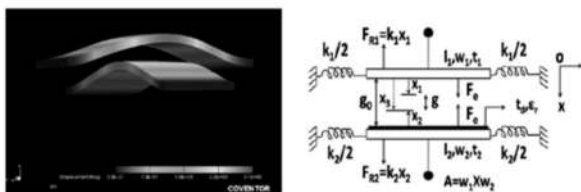


Figure 7: RF MEMS switch with movable electrode and mechanical model [89]

3.2.2 Reduction of residual stress

The second parameter is the effect of tensile residual stress on the spring constant during the fabrication process [90]. It causes the beam to deflect upward, therefore it increases the actuation voltage. The residual stress can be reduced by different techniques. The first method is the cancelling of the residual stress by using different micro structures. Zhiao et al. [91] reported a RF MEMS series switch for DC to X band which used Al/Au slant beam at the end of the cantilever. This composite beam is able to cancel the bending moment. The actuation voltage of this switch is 40V. Ur Rahman et al. [92] used a dimple at the end of the beam to overcome the residual stress. The contact of this switch is DC and it is fabricated on Alumina with a CPW transmission line for the frequencies of DC-40

GHz. The actuation voltage of the switch is 19V. Chan et al. [93] designed an inline low actuation voltage by reducing the sensitivity of the beam to residual stress through applying corrugations to their beam. This switch is a DC contact series RF MEMS switch with an actuation voltage of 20V. This switch is supported at two anchor points. It also has four springs which are connected at one end to an anchor and at the other end to the centre beam.

The second method to reduce the residual stress is through low-stress fabrication processes. Gong et al. (2009) developed a flat cantilever for 2-75GHz. They used an Al base sacrificial layer instead of a polymer sacrificial layer to reduce the stress gradient for the gold membrane. This is due to the coefficient of thermal expansion (CTE) between Al and Au (21 and 14ppm/K), respectively, rather than the typical polymer materials such as photoresist (>50ppm/K). The actuation voltage of this switch is still high and more than 40V. Biyikli et al. [94] reported a DC contact RF MEMS series switch with a frequency band from 0 to 25GHz. The gap between the transmission line and the beam is controlled by the amount of internal stress gradient. Tuning of the stress gradient depends on the decrease and increase of pressure for the bottom half, which results in a compressive stressed layer, and increase of the pressure for the top half layer for achieving the tensile stress. This leads to a compressive and tensile stress for the bottom and top layers. This experiment was done on different sizes of cantilever with the length ($L=5-50\mu\text{m}$) and width ($W=2-40\mu\text{m}$). The actuation voltage of all switches in this experiment is less than 20V.

3.3 Reduction of size (carbon switches)

Carbon switches can be fabricated in the range of nm, therefore, this type of switches is mostly named as NEMS switches. The rule for calculation of mechanical and RF parameters of carbon switches follows the rule of MEMS switches. The only difference between the MEMS and the NEMS switches is the role of Van der Waals force (Figure 2). A dynamic and mechanical study on the CNT NEMS switch is presented in [95-97]. The actuation voltage of the NEMS switches based on CNT and graphene is given as bellow:

For CNT:

$$V_{pull-in} = \sqrt{\left[k(g - g_{eq}) - \frac{\pi C_6 \rho^2 \omega L}{6} \left(\frac{1}{g_{eq}^3} - \frac{1}{(g_{eq} + t)^3} \right) \right] \times \frac{2g_{eq}^2}{\left(1 + \frac{2g_{eq}}{\pi \omega} \right) \omega L \epsilon_0}} \tag{9}$$

where g is the gap between the conductor and the ground, C_6 is a constant characterizing the interac-

tions between the two atoms, ρ is the volume density of graphite, which is taken to be $\rho = 1.14 \times 10^{29} \text{ m}^{-3}$, and $g_{eq} = 2/3g_0$.

For Graphene:

$$V_{pull-in} = \sqrt{\frac{8kg_0^3}{27\epsilon WL} - \frac{A_h}{2\pi\epsilon g_0}} \tag{10}$$

where A_h is the Hamaker constant (1.579eV), W and L are physical dimension of cantilever

The first term in the Equation (10) represents the contribution of the electrostatic force and the second term refers to the contribution of the Van der Waals force.

The first type of CNT NEMS switch is a dual fixed type switch. Kaul et al. [98] reported on a dual fixed capacitive RF NEMS switch based on SWCNT. The actuation voltage of the switch is less than 5V and the switching time is 2.8ns. The size of the SWCNT beam is 200nm long, and with a diameter of 2nm, and a gap of 20nm. The Young’s modulus for this switch is 1Tpa. Acquaviva et al. [64] reported on a dual fixed capacitive RF NEMS switch based on SWCNT arrays for membrane. The actuation voltage of this switch is 6V. The resistivity of the beam is reported as 0.0077 $\Omega \cdot \text{cm}$ and the flexural Young’s modulus is very low (8.5 GPa). This is due to the fact that only a small portion of CNT contributes as a membrane and shear modulus during the actuation. A very low actuation voltage and fast dual fixed type RF NEMS switch is reported by Dragoman et al. [99]. The actuation voltage of this switch is less than 1 volt and its switching time is 100ps.

Another type of RF NEMS switch is the cantilever type RF NEMS switch. Dragoman et al. [99] reported on a RF cantilever NEMS switch which used 4 vertical CNT cantilevers based on the CPW as a nanotweezer switch. Each two cantilevers are attracted by applying a DC voltage across them and forming a short circuit. The length of CNT tweezers is 2.5 μm . The actuation voltage for this switch is 14.5V, and is higher than other report-

ed CNT NEMS switches. This is due to the low Van der Waals force. As discussed before, Van der Waals force is only effective in nm gaps. The switching time for this switch is 49ns. Lee et al. [100] reported on a cantilever type RF NEMS switch based on MWCNT. The actuation voltage of this switch is less than 5V. The CNT has a 0.5nm diameter and is 1.8 μm long. The gap between the transmission line and the CNT cantilever is 150nm. This switch used gold as a bottom electrode and Au/Ti (70/5nm) for CNT contact.

Milaninia et al. [101] presented the NEMS switch with two layers of graphene. Therefore, two CVD processes were used. The size of the beam is 20 \times 3 μm ($L \times w$) and $g = 500\text{nm}$. The actuation voltage is 4.5V. The main disadvantage of this switch is a limitation of contact resistance between the top and bottom graphene layers (200k Ω). This is due to the nonuniform surface of the CVD grown graphene. Dragoman et al. [102, 103] simulated a double clamped RF NEMS switch based on a graphene membrane. 20nm gold is patterned on 500 μm Si to form a CPW transmission line. The gap between the signal line and the membrane is 1 μm . The CPW is loaded by the number of graphene flakes with a width of 0.6 μm . This switch can be used for 1-60GHz applications. Increasing the number of graphene membranes above the TL increases the performance of the switch in the down state position, but it does not affect it on the up state position. The actuation voltage of this switch is 2V. The main drawback of all the discussed RF NEMS switches is the insertion loss and isolation in up and down state positions, respectively.

4 Discussion

As described in Section 3, the actuation voltage of the RF MEMS can be reduced by using three methods. Table 5 compares the impacts of these three methods on both mechanical and RF parameters of the switches.

Impacts on Actuation voltage

Table 5 compares the effect of each method on the actuation voltage of RF MEMS switches. As can be seen

Table 5: Comparison of low actuation methods on mechanical and RF parameters

Methods	Parameters	Vpull-in	RF parameters	Switching time	Fabrication process	Reduction of size
Reduction of Spring constant	Beam	Low	Good	Slow	Hard	Medium
	Residual stress	High	Good	Slow	Hard	Medium
Reduction of Gap	Matching circuit	Low	Very Good	Good	Good	Large
	Torsional actuation	Low	Good	Good	Good	Large
	Comb structure	Low	Good	Very Slow	Simple	Very large
Reduction of Size	Carbon Nano tube	Extremely Low	Not Good	Extremely fast	Extremely Hard	Small
	Graphene	Extremely Low	Not Good	Extremely Fast	Extremely hard	Small

from the table, carbon switches have the lowest actuation voltage. Decreasing the size has a negative impact on the actuation voltage but because of the presence of the Van der Waals force in the range of nm, this type of switches has the lowest actuation voltage. The second method that has the highest impact on lowering the actuation voltage is reduction of the gap because the relation between the gap and the actuation voltage is more than other parameters ($V_{pull-in} \propto g^{\frac{3}{2}}$). The last method is to reduce the spring constant. This method has the lowest impact on the actuation voltage ($V_{pull-in} \propto K^{\frac{1}{2}}$).

RF parameters

Table 5 compares the effects of each method on the RF parameters. The first parameter is reduction of the gap. The RF parameters of the switch strongly depend on the amount of capacitance in the up and down states. As presented in Table 4, the reduction of the gap has a negative impact on RF parameters. This problem is resolved by the techniques that were reviewed in Section 3. For example, compensation of the parasitic capacitance by matching impedance, providing a large contact area and a large gap by torsional actuations or increasing the force by lateral comb driver. These techniques are used to reduce the gap with acceptable RF parameters. Also, low actuation can be achieved by reducing the K without any effect on the amount of capacitance and RF parameters. The RF parameters of NEMS switches are not good for the microwave frequency but this may change in the future.

Switching time

Table 5 compares the effects of each method on switching time. NEMS switches based on CNT and Graphene have the highest speed due to the high Young's modulus of CNT and graphene, which is 1TPa. It is reported that the speed of the NEMS switches is in the range of a few tens of nano seconds and even equal to or faster than semiconductor switches [99, 104]. Using torsional and matching impedances does not have an effect on the speed of switches, and this is the same method used for other types of conventional RF MEMS switches. But comb structures are very slow because all actuators, transmission lines and beams are connected to each other, and therefore the membrane is very heavy compared to other type of MEMS switches. Reducing the spring constant also impacts negatively on the speed of the switch.

Size of switch

Table 5 compares the size of the RF MEMS switches. It is obvious that the size of RF NEMS switches is smaller than the MEMS switches. Lowering the spring constant does not affect the size of switches. However, methods

for lowering the actuation voltage by decreasing the gap increase the size of MEMS switches. This is due to the micro structures that they use for reducing the actuation voltage. For example, a comb structure has the largest size because of the drivers. Moreover, reduction of the gap by using matching circuits uses additional space on the transmission line due to the presence of SHITL. Torsional actuation has a large area due to the pillars, extra electrodes and additional voltage source.

Fabrication and set up

The fabrication process of RF MEMS switches based on CNT and Graphene is different to that of conventional RF MEMS switches and is more sophisticated than that used for conventional MEMS switches. Also, CNT and graphene are more expensive than other metal materials.

The fabrication process for reduction of the gap is categorized into three methods. The first method for reduction of the gap uses matching impedance. The fabrication of this type exactly follows the fabrication of the RF MEMS switch and there is no additional process for it. The second group uses torsional actuation. It requires more fabrication processing than the normal process for MEMS switches. For example, the switch which is fabricated by Touati et al. [80] used nine masks and RIE etching for patterning pillars. Moreover, it requires two voltage sources to provide positive and negative voltages. The third type is comb switches. The fabrication process is less complex than other types of MEMS switches because actuator, transmission line and beam are all fabricated in one step of lithography. However, the gap demands RIE etching instead of wet etching. Moreover, most of the reported RF MEMS comb switches are DC contact and there is less capacitive MEMS shunt switches reported with comb structures. This is due to the deposition of dielectric on the side walls which limits the On and Off capacitance ratio. The existing capacitance RF MEMS comb switches were fabricated by Park et al. [88], where air was used as dielectric material. He et al. [85] used paryline material instead of air.

The methods for reduction of spring constant can be categorized in two groups. The first method uses different types of micro structures such as pillars or corrugation to cancel the curling. It requires an additional fabrication process. The second method is fabrication of MEMS switches via low residual stress material. The main disadvantage of this method is the complexity of measuring the amount of residual stress. This is because it requires determination of the exact amount of residual stress on each step such as lithography and deposition of materials.

5 Conclusion

In this paper, methods for the reduction of the actuation voltage of RF MEMS electrostatic switches have been studied. The study was conducted based on various experiments and analysis presented in recent published works. Electrostatic MEMS/NEMS switches are categorized based on their materials into metallic and carbon switches. Reduction of gap and spring constant are mostly used for reducing the actuation voltage of RF MEMS switches based on metals. The fabrication of this type of switches is based on surface micromachining. Switches based on CNT and graphene, NEMS switches, are fabricated in nano sizes. They are a new generation of electro-mechanical switches, and researchers are trying to improve their RF parameters. The fabrication of this type of switches is based on the CVD process. The impact of this method has been analysed and briefly discussed according to the mechanical parameters and RF parameters, taking into account the fabrication process. The materials presented in this paper enable researchers to better optimize their design based on the available fabrication facility and the desired application.

References

- Lucyszyn, S., *Advanced RF Mems*, 2010. (New York: Cambridge University Press).
- Rebeiz, G.M., *RF MEMS*, 2003. Wiley Online Library).
- Gammel, P., G. Fischer and J. Bouchaud, *RF MEMS and NEMS technology, devices, and applications*, Bell Labs Technical Journal, 2005. 10. p. 29-59.
- Rebeiz, G., K. Entesari, I. Reines, S.J. Park, M. El-Tanani, A. Grichener and A. Brown, *Tuning in to RF MEMS*, *Microwave Magazine, IEEE*, 2009. 10. p. 55-72.
- Jones, R. and M. Chapman, *RF MEMS in mobile phones*, *RF DESIGN*, 2005. 28. p. 20.
- Gu, Q. and J.R. De Luis. *RF MEMS tunable capacitor applications in mobile phones*. 2010. IEEE.
- Kolb, S., *MEMS PRODUCTS AND MEMS TECHNOLOGIES FOR AUTOMOTIVE APPLICATIONS AT INFENION*, *INFORMACIJ MIDEM*, 2006. 36. p. 185-189.
- Drago Strle, V.K., *MEMS BASED INERTIAL SYSTEMS*, *INFORMACIJ MIDEM*, 2007. 37. p. 11.
- Mortazavi, D., A.Z. Kouzani, Y. Mafinejad and M. Hosain. *Plasmon eigenvalues as a function of nano-spheroids size and elongation*. *Complex Medical Engineering (CME)*, 2012 ICME International Conference on, 2012. IEEE.
- Khoshmanesh, K., A.Z. Kouzani, S. Nahavandi, S. Baratchi and J. Kanwar, *Design and simulation of an interdigital-chaotic advection micromixer for lab-on-a-chip applications*, *La houille blanche*, 2009. 118-124.
- Tehranirokh, M., A.Z. Kouzani, P.S. Francis and J.R. Kanwar, *Generating different profiles of gradient concentrations inside a gel-filled chamber: design and simulation*, *Microsystem technologies*, 2012. 1-6.
- Islam, M., A.Z. Kouzani, X.J. Dai, W.P. Michalski and H. Gholamhosseini, *Design and Analysis of a Multilayer Localized Surface Plasmon Resonance Graphene Biosensor*, *Journal of Biomedical Nanotechnology*, 2012. 8. p. 380-393.
- Daneshmand, M. and R. Mansour, *RF MEMS Satellite Switch Matrices*, *Microwave Magazine, IEEE*, 2011. 12. p. 92-109.
- Malmqvist, R., C. Samuelsson, B. Carlegrim, P. Rantakari, T. Vähä-Heikkilä, A. Rydberg and J. Varis. *Ka-band RF MEMS phase shifters for energy starved millimetre-wave radar sensors*. 2010. IEEE.
- Fox, C.H., X. Chen, H.W. Jiang, P.B. Kirby and S. McWilliam. *Development of micromachined RF switches with piezofilm actuation*. 2002.
- Polcawich, R.G., J.S. Pulskamp, D. Judy, P. Ranade, S. Trolrier-McKinstry and M. Dubey, *Surface micromachined microelectromechanical ohmic series switch using thin-film piezoelectric actuators*, *Microwave Theory and Techniques, IEEE Transactions on*, 2007. 55. p. 2642-2654.
- Gross, S., S. Tadigadapa, T. Jackson, S. Trolrier-McKinstry and Q. Zhang, *Lead-zirconate-titanate-based piezoelectric micromachined switch*, *Applied Physics Letters*, 2003. 83. p. 174-176.
- Guerre, R., U. Drechsler, D. Bhattacharyya, P. Rantakari, R. Stutz, R.V. Wright, Z.D. Milosavljevic, T. Vaha-Heikkila, P.B. Kirby and M. Despont, *Wafer-level transfer technologies for PZT-based RF MEMS switches*, *Journal of Microelectromechanical Systems*, 2010. 19. p. 548-560.
- Proie, R.M., R.G. Polcawich, J.S. Pulskamp, T. Ivanov and M.E. Zaghoul, *Development of a PZT MEMS Switch Architecture for Low-Power Digital Applications*, *Microelectromechanical Systems, Journal of*, 2011. 20. p. 1032-1042.
- Polcawich, R.G., D. Judy, J.S. Pulskamp, S. Trolrier-McKinstry and M. Dubey. *Advances in Piezoelectrically Actuated RF MEMS Switches and Phase Shifters*. *Microwave Symposium*, 2007. IEEE/MTT-S International, 2007.
- Mahameed, R., N. Sinha, M.B. Pisani and G. Piazza, *Dual-beam actuation of piezoelectric AlN RF MEMS switches monolithically integrated with AlN contour-mode resonators*, *Journal of Micro-*

- mechanics and Microengineering, 2008. 18. p. 105011.
22. Klaasse, G., R. Puers and H. Tilmans, Piezoelectric versus electrostatic actuation for a capacitive RF-MEMS switch, *Proc. SeSens*, 2002. 631-634.
 23. Lee, T.M., Y.H. Seo, K.H. Whang and D.S. Choi, Study on the Lateral Piezoelectric Actuator with Actuation Range Amplifying Structure, *Key Engineering Materials*, 2006. 326. p. 289-292.
 24. Il-Joo, C., S. Taeksang, B. Sang-Hyun and Y. Euisik, A low-voltage and low-power RF MEMS series and shunt switches actuated by combination of electromagnetic and electrostatic forces, *Microwave Theory and Techniques, IEEE Transactions on*, 2005. 53. p. 2450-2457.
 25. Cho, I.J. and E. Yoon, Design and fabrication of a single membrane push-pull SPDT RF MEMS switch operated by electromagnetic actuation and electrostatic hold, *Journal of Micromechanics and Microengineering*, 2010. 20. p. 035028.
 26. Zhang, Y., G. Ding, X. Shun, D. Gu, B. Cai and Z. Lai, Preparing of a high speed bistable electromagnetic RF MEMS switch, *Sensors and Actuators A: Physical*, 2007. 134. p. 532-537.
 27. Nordquist, C.D., M.S. Baker, G.M. Kraus, D.A. Czaplowski and G.A. Patrizi, Poly-Silicon Based Latching RF MEMS Switch, *IEEE Microwave and Wireless Components Letters*, 2009. 19. p. 380-382.
 28. de los Santos, H.J., G. Fischer, H.A.C. Tilmans and J.T.M. Van Beek, RF MEMS for ubiquitous wireless connectivity. Part I. Fabrication, *Microwave Magazine, IEEE*, 2004. 5. p. 36-49.
 29. Balachandran, S., J. Kusterer, D. Maier, M. Dipalo, T. Weller and E. Kohn. High power nanocrystalline diamond RF MEMS- A combined look at mechanical and microwave properties. *Microwaves, Communications, Antennas and Electronic Systems*, 2008. COMCAS 2008. IEEE International Conference on, 2008.
 30. Seong-Dae, L., J. Byoung-Chul, S.D. Kim and R. Jin-Koo, A novel pull-up type RF MEMS switch with low actuation voltage, *Microwave and Wireless Components Letters, IEEE*, 2005. 15. p. 856-858.
 31. Mansour, R., M. Bakri-Kassem, M. Daneshmand and N. Messiha. RF MEMS devices. 2003. IEEE.
 32. Ruan, J., G.J. Papaioannou, N. Nolhier, M. Bafleur, F. Coccetti and R. Plana. ESD stress in RF-MEMS capacitive switches: The influence of dielectric material deposition method. *Reliability Physics Symposium, 2009 IEEE International*, 2009.
 33. Malmqvist, R., C. Samuelsson, W. Simon, P. Rantakari, D. Smith, M. Lahdes, M. Lahti, Va, x, ha, Heikkila, T., J. Varis and R. Baggen. Design, packaging and reliability aspects of RF MEMS circuits fabricated using a GaAs MMIC foundry process technology. *Microwave Conference (EuMC), 2010 European*, 2010.
 34. Das, C.K., P. Bhattacharya and S.S. Kalra, Graphene and MWCNT: Potential Candidate for Microwave Absorbing Materials, *Journal of Materials Science Research*, 2012. 1. p. p126.
 35. Dragoman, M., D. Neculoiu, D. Dragoman, G. Deligeorgis, G. Konstantinidis, A. Cismaru, F. Coccetti and R. Plana, Graphene for Microwaves, *Microwave Magazine, IEEE*, 2010. 11. p. 81-86.
 36. Liao, M. and Y. Koide, Carbon-Based Materials: Growth, Properties, MEMS/NEMS Technologies, and MEM/NEM Switches, *Critical Reviews in Solid State and Materials Sciences*, 2011. 36. p. 66-101.
 37. Saberi, M., R. Lotfi, K. Mafinezhad and W.A. Serdijn, Analysis of power consumption and linearity in capacitive digital-to-analog converters used in successive approximation ADCs, *Circuits and Systems I: Regular Papers, IEEE Transactions on*, 2011. 58. p. 1736-1748.
 38. Saberi, M., H. Sepehrian, R. Lotfi and K. Mafinezhad, A low-power Successive Approximation ADC for biomedical applications, *IEICE electronics express*, 2011. 8. p. 195-201.
 39. Mafinezhad, K., Modeling and optimisation of a solenoidal integrated inductor for RFICs, *International journal of RF and Microwave Computer-Aided Engineering*, 2009. 5. p.
 40. Mafinezhad, K. and S.H. Keshmiri, Design and Simulation of an Oblique Suspender MEMS Variable Capacitor, *Scientia Iranica*, 2006. 13. p.
 41. Nabovati, H., K. Mafinezhad, A. Nabovati and H. Keshmiri, Comprehensive Electromechanical Analysis of MEMS Variable Gap Capacitors, *JOURNAL OF IRANIAN ASSOCIATION OF ELECTRICAL AND ELECTRONICS ENGINEERS*, 2007. 4. p. 3.
 42. Daliri, M., M. Maymandi-Nejad and K. Mafinezhad, Distortion analysis of bootstrap switch using voltterra series, *Circuits, Devices & Systems, IET*, 2009. 3. p. 359-364.
 43. Fedder, G.K., R.T. Howe, T.J.K. Liu and E.P. Quévy, Technologies for cofabricating MEMS and electronics, *Proceedings of the IEEE*, 2008. 96. p. 306-322.
 44. Kris Baert, C.V.H., *Integrated Microsystems, Informacij MIDEM*, 2006. 36. p. 7.
 45. Becker, J., Configurability for Systems on Silicon: Requirement and Perspective for future VLSI Solutions, *INFORMACIJE MIDEM-LJUBLJANA-*. 2003. 33. p. 236-244.
 46. Lee, M.J., Y. Zhang, C. Jung, M. Bachman, F. De Flaviis and G. Li, A novel membrane process for RF MEMS switches, *Microelectromechanical Systems, Journal of*, 2010. 19. p. 715-717.
 47. Goldsmith, C.L., Z. Yao, S. Eshelman and D. Denniston, Performance of low-loss RF MEMS capacitive

- switches, *Microwave and Guided Wave Letters*, IEEE, 1998. 8. p. 269-271.
48. Lakshminarayanan, B. and T.M. Weller, Design and modeling of 4-bit slow-wave MEMS phase shifters, *Microwave Theory and Techniques*, IEEE Transactions on, 2006. 54. p. 120-127.
 49. Mercier, D., K. Van Caekenbergh and G.M. Rebeiz. Miniature RF MEMS switched capacitors. 2005. IEEE.
 50. G.Nassiopoulou, A., POROUS SILICON FOR SENSORS AND ON-CHIP INTEGRATION OF RF COMPONENT, *Informacij MIDEM*, 2006. 36. p. 7.
 51. Ding, Y., Z. Liu, L. Liu and Z. Li, A surface micromachining process for suspended RF-MEMS applications using porous silicon, *Microsystem technologies*, 2003. 9. p. 470-473.
 52. Guo, F., Z. Zhu, Y. Long, W. Wang, S. Zhu, Z. Lai, N. Li, G. Yang and W. Lu, Study on low voltage actuated MEMS rf capacitive switches, *Sensors and Actuators A: Physical*, 2003. 108. p. 128-133.
 53. Meyyappan, M., *Carbon nanotubes: science and applications*, 2005. CRC).
 54. Dresselhaus, M.S., G. Dresselhaus and P. Eklund, *Science of fullerenes and carbon nanotubes*, 1996. Academic Pr).
 55. Dubois, S.M.M., Z. Zanolli, X. Declerck and J.C. Charlier, Electronic properties and quantum transport in Graphene-based nanostructures, *The European Physical Journal B-Condensed Matter and Complex Systems*, 2009. 72. p. 1-24.
 56. Bolotin, K.I., K. Sikes, Z. Jiang, M. Klima, G. Fudenberg, J. Hone, P. Kim and H. Stormer, Ultrahigh electron mobility in suspended graphene, *Solid State Communications*, 2008. 146. p. 351-355.
 57. Teo, K., M. Chhowalla, G. Amaratunga, W. Milne, D. Hasko, G. Pirio, P. Legagneux, F. Wyczisk and D. Pribat, Uniform patterned growth of carbon nanotubes without surface carbon, *Applied Physics Letters*, 2001. 79. p. 1534.
 58. Gad-el-Hak, M., *MEMS: design and fabrication*, 2006, 2. CRC press).
 59. Rahman, H.U., *Plasma Based Dry Release of MEMS Devices*.
 60. Yo-Tak, S., L. Hai-Young and M. Esashi, Low actuation voltage capacitive shunt RF-MEMS switch having a corrugated bridge, *IEICE transactions on electronics*, 2006. 89. p. 1880-1887.
 61. Giacomozzi, F., V. Mulloni, S. Colpo, J. Iannacci, B. Margesin and A. Faes, A Flexible Fabrication Process for RF MEMS Devices, *Romanian Journal of Information Science and Technology (ROMJIST)*, 2011. 14. p. 259-268.
 62. Iliescu, C., MICROFLUIDICS IN GLASS: TECHNOLOGIES AND APPLICATIONS, *Informacij MIDEM*, 2006. 36. p. 7.
 63. Alireza Bahadorimehr, B.Y.M., FABRICATION OF GLASS-BASED MICROFLUIDIC DEVICES WITH PHOTORESIST AS MASK, *Informacij MIDEM*, 2011. 41. p. 4.
 64. Acquaviva, D., A. Arun, S. Esconjauregui, D. Bouvet, J. Robertson, R. Smajda, A. Magrez, L. Forro and A. Ionescu, Capacitive nanoelectromechanical switch based on suspended carbon nanotube array, *Applied Physics Letters*, 2010. 97. p. 233508.
 65. Cassell, A.M., N.R. Franklin, T.W. Tomblor, E.M. Chan, J. Han and H. Dai, Directed growth of free-standing single-walled carbon nanotubes, *Journal of the American Chemical Society*, 1999. 121. p. 7975-7976.
 66. Mahshid Kalani, R.Y., carbon nano tube via chemical vapour deposition, *Asian Journal of Chemistry*, 2011. 23. p. 4735-4743.
 67. Dequesnes, M., S. Rotkin and N. Aluru, Calculation of pull-in voltages for carbon-nanotube-based nanoelectromechanical switches, *Nanotechnology*, 2002. 13. p. 120.
 68. Dequesnes, M., Z. Tang and N. Aluru, Static and dynamic analysis of carbon nanotube-based switches, *Journal of engineering materials and technology*, 2004. 126. p. 230.
 69. Kang, J.W., S.C. Kong and H.J. Hwang, Electromechanical analysis of suspended carbon nanotubes for memory applications, *Nanotechnology*, 2006. 17. p. 2127.
 70. Lucyszyn, S., *Advanced RF MEMS 2010*. Cambridge University Press).
 71. Rebeiz, G.M., *RF MEMS: Theory, Design, and Technology*, 2003.
 72. Varadan, V.K., *RF MEMS and their applications 2002*, Wiley: New York.
 73. Younis, M.I., *Sensing and Actuation in MEMS, MEMS Linear and Nonlinear Statics and Dynamics*, 2011. 57-96.
 74. Reinhold Ludwig, G.B., *RF circuit design : theory and applications 2009*. Prentice-Hall).
 75. Mafinejad, Y., A.Z. Kouzani, K. Mafinezhad and A. Golmakani, Pi-shaped MEMS architecture for lowering actuation voltage of RF switching, *IEICE electronics express*, 2009. 6. p. 1483-1489.
 76. Mafinejad, Y., K. Mafinezhad and A.Z. Kouzani, Improving RF characteristics of MEMS capacitive shunt switches, *International Review of Modeling and Simulations (IREMOS)*, 2009.
 77. Mafinejad, Y., A.Z. Kouzani, K. Mafinezhad and H. Nabovatti. Design and simulation of a low voltage wide band RF MEMS switch. *International Conference on Systems, Man and Cybernetics San Antonio, Texas, USA*, 2009. IEEE.
 78. Mafinejad, Y., A.Z. Kouzani, K. Mafinezhad and A. Kaynak, Low Actuation Wideband RF MEMS

- Shunt Capacitive Switch, *Procedia Engineering*, 2012. 29. p. 1292-1297.
79. Zarghami, M., Y. Mafinejad, A. Kouzani and K. Mafinezhad, Low actuation-voltage shift in MEMS switch using ramp dual-pulse, *IEICE electronics express*, 2012. 9. p. 1062-1068.
 80. Touati, S., N. Lorphelin, A. Kancierzewski, R. Robin, A.S. Rollier, O. Millet and K. Segueni. Low actuation voltage totally free flexible RF MEMS switch with antistiction system. 2008. IEEE.
 81. Robin, R., S. Touati, K. Segueni, O. Millet and L. Buchailot. A new four states high deflection low actuation voltage electrostatic MEMS switch for RF applications. 2008. IEEE.
 82. Kim, C., Mechanically Coupled Low Voltage Electrostatic Resistive RF Multi-throw Switch, *IEEE Transactions on Industrial Electronics*, 2011. 1-1.
 83. Liu, A., M. Tang, A. Agarwal and A. Alphones, Low-loss lateral micromachined switches for high frequency applications, *Journal of Micromechanics and Microengineering*, 2005. 15. p. 157.
 84. He, X., B. Liu, Z. Lv and Z. Li, A lateral RF MEMS capacitive switch utilizing parylene as dielectric, *Microsystem Technologies*, 2012. 1-9.
 85. He, X., B. Liu, Z. Lv and Z. Li, A lateral RF MEMS capacitive switch utilizing parylene as dielectric, *Microsystem Technologies*, 2011. 1-9.
 86. Kang, S., H.C. Kim and K. Chun. Single pole four throw RF MEMS switch with double stop comb drive. 2008. IEEE.
 87. Akiba, A., S. Mitarai, S. Morita, K. Ikeda, S. Kurth, S. Leidich, A. Bertz, M. Nowack, J. Froemel and T. Gessner. A fast and low actuation voltage MEMS switch for mm-wave and its integration. 2010. IEEE.
 88. Park, J., E.S. Shim, W. Choi, Y. Kim, Y. Kwon and D. Cho, A Non-Contact-Type RF MEMS switch for 24-GHz radar applications, *Journal of Microelectromechanical Systems*, 2009. 18. p. 163-173.
 89. Kundu, A., S. Sethi, N. Mondal, B. Gupta, S. Lahiri and H. Saha, Analysis and optimization of two movable plates RF MEMS switch for simultaneous improvement in actuation voltage and switching time, *Microelectronics Journal*, 2010. 41. p. 257-265.
 90. Huang, J.M., K.M. Liew, C.H. Wong, S. Rajendran, M.J. Tan and A.Q. Liu, Mechanical design and optimization of capacitive micromachined switch, *Sensors and Actuators A: Physical*, 2001. 93. p. 273-285.
 91. Zhihao, H., L. Zewen and L. Zhijian. Al/Au composite membrane bridge DC-contact series RF MEMS switch. *Solid-State and Integrated-Circuit Technology*, 2008. ICSICT 2008. 9th International Conference on, 2008.
 92. Rahman, H.U. and R. Ramer. Supported bars novel cantilever beam design for RF MEMS series switches. 2009. IEEE.
 93. Chan, K.Y. and R. Ramer. RF MEMS Switch with low stress sensitivity and low actuation voltage. 2009. IEEE.
 94. Biyikli, N., Y. Damgaci and B. Cetiner, Low-voltage small-size double-arm MEMS actuator, *Electronics Letters*, 2009. 45. p. 354-356.
 95. Shi, Z., H. Lu, L. Zhang, R. Yang, Y. Wang, D. Liu, H. Guo, D. Shi, H. Gao and E. Wang, Studies of graphene-based nanoelectromechanical switches, *Nano Research*, 2011. 1-6.
 96. Fujita, S., K. Nomura, K. Abe and T.H. Lee, 3-d nanoarchitectures with carbon nanotube mechanical switches for future on-chip network beyond cmos architecture, *Circuits and Systems I: Regular Papers, IEEE Transactions on*, 2007. 54. p. 2472-2479.
 97. Rajter, R., R. French, W. Ching, W. Carter and Y. Chiang, Calculating van der Waals-London dispersion spectra and Hamaker coefficients of carbon nanotubes in water from ab initio optical properties, *Journal of Applied Physics*, 2007. 101. p. 054303.
 98. Kaul, A.B., E.W. Wong, L. Epp and B.D. Hunt, Electromechanical carbon nanotube switches for high-frequency applications, *Nano letters*, 2006. 6. p. 942-947.
 99. Dragoman, M., A. Takacs, A. Muller, H. Hartnagel, R. Plana, K. Grenier and D. Dubuc, Nanoelectromechanical switches based on carbon nanotubes for microwave and millimeter waves, *Applied Physics Letters*, 2007. 90. p. 113102-113102-3.
 100. Lee, S.W., D.S. Lee, R.E. Morjan, S.H. Jhang, M. Sveningsson, O. Nerushev, Y.W. Park and E.E.B. Campbell, A three-terminal carbon nanorelay, *Nano letters*, 2004. 4. p. 2027-2030.
 101. Milaninia, K.M., M.A. Baldo, A. Reina and J. Kong, All graphene electromechanical switch fabricated by chemical vapor deposition, *Applied Physics Letters*, 2009. 95. p. 183105.
 102. Dragoman, M., D. Dragoman, F. Coccetti, R. Plana and A. Muller, Microwave switches based on graphene, *Journal of Applied Physics*, 2009. 105. p. 054309-054309-3.
 103. Dragoman, M., D. Dragoman and A. Muller. High frequency devices based on graphene. 2007. IEEE.
 104. Frank, I., D. Tanenbaum, A. Van Der Zande and P. McEuen, Mechanical properties of suspended graphene sheets, *Journal of Vacuum Science & Technology B: Microelectronics and Nanometer Structures*, 2007. 25. p. 2558.

Received: 27. 08. 2012

Accepted: 27. 05. 2013